Biochemical Pharmacology 83 (2012) 723–732

Contents lists available at SciVerse ScienceDirect

Biochemical Pharmacology

journal homepage: www.elsevier.com/locate/biochempharm

Hydrogen sulfide-releasing aspirin suppresses NF-κB signaling in estrogen receptor negative breast cancer cells in vitro and in vivo

Mitali Chattopadhyay [a], Ravinder Kodela [a], Niharika Nath [b], Arpine Barsegian [a], Daniel Boring [c], Khosrow Kashfi [a,*]

[a] Department of Physiology and Pharmacology, Sophie Davis School of Biomedical Education, City University of New York Medical School, New York, NY 10031, United States
[b] Department of Life Sciences, New York Institute of Technology, New York, NY 10023, United States
[c] Division of Cancer Prevention, National Cancer Institute, Bethesda, MD 20892, United States

ARTICLE INFO

Article history:
Received 14 September 2011
Accepted 15 December 2011
Available online 24 December 2011

Keywords:
Hydrogen sulfide
Estrogen receptor negative breast cancer
NF-κB
Thioredoxin reductase
Chemoprevention

ABSTRACT

Hormone-dependent estrogen receptor positive (ER+) breast cancers generally respond well to anti-estrogen therapy. Unfortunately, hormone-independent estrogen receptor negative (ER−) breast cancers are aggressive, respond poorly to current treatments and have a poor prognosis. New approaches and targets are needed for the prevention and treatment of ER− breast cancer. The NF-κB signaling pathway is strongly implicated in ER− tumor genesis, constituting a possible target for treatment. Hydrogen sulfide-releasing aspirin (HS-ASA), a novel and safer derivative of aspirin, has shown promise as an anti-cancer agent. We examined the growth inhibitory effect of HS-ASA via alterations in cell proliferation, cell cycle phase transitions, and apoptosis, using MDA-MB-231 cells as a model of triple negative breast cancer. Tumor xenografts in mice, representing human ER− breast cancer, were evaluated for reduction in tumor size, followed by immunohistochemical analysis for proliferation, apoptosis and expression of NF-κB. HS-ASA suppressed the growth of MDA-MB-231 cells by induction of G_0/G_1 arrest and apoptosis, down-regulation of NF-κB, reduction of thioredoxin reductase activity, and increased levels reactive oxygen species. Tumor xenografts in mice, were significantly reduced in volume and mass by HS-ASA treatment. The decrease in tumor mass was associated with inhibition of cell proliferation, induction of apoptosis and decrease in NF-κB levels in vivo. HS-ASA has anti-cancer potential against ER− breast cancer and merits further study.

1. Introduction

Breast cancer is one of the most common malignancies among women [1,2]. The treatment of breast cancer usually relies on surgery and radiotherapy and/or chemotherapeutic drugs. Estrogen receptor positive breast cancers generally have a better prognosis and are often responsive to anti-estrogen therapy [3]. Unfortunately, estrogen receptor negative breast cancers are more aggressive [4] and unresponsive to anti-estrogens. Triple negative breast cancers (TNBC) lack expression of estrogen receptor (ER) and progesterone receptor (PR), and do not over-express HER2, and are treated mainly by cytotoxic chemotherapy [5]. For TNBCs, there is an urgent need to develop novel anticancer agents with low cytotoxic effects, and which can effectively inhibit tumor cell proliferation pathways [6,7].

NSAIDs are important agents for cancer prevention and may serve as possible adjunct in cancer treatment based on reports that they stimulate anticancer effects in vitro, inhibit carcinogenesis in carcinogen-induced and genetically driven rodent models, reduce the incidence of colorectal precancerous lesions and colon cancer incidence, and regress precancerous lesions in genetic and sporadic cancer risk cohorts [8–12]. However, NSAID-induced upper gastrointestinal side effects remain a major problem that affects a broad segment of the population, due to frequent prescription and over the counter dispensing [13]. These reasons have stimulated the search for alternative anti-inflammatory drugs that are safe for long-term use. Hydrogen sulfide (H_2S), recently hypothesized as the third 'gasotransmitter' alongside nitric oxide and carbon monoxide, has been attracting extensive attention because of its multiple physiological and pathophysiological roles in various body systems [14–16]. The H_2S-releasing derivative of mesalamine has demonstrated superior anti-inflammatory and anti-nociceptive efficacy compared with the base mesalamine molecule in a rodent experimental model of colitis-associated colorectal distension [17]. Recently, it was reported that H_2S-releasing diclofenac inhibited lipopolysaccharide-induced

* Corresponding author at: Department of Physiology and Pharmacology, City University of New York Medical School, 138th Street and Convent Avenue, New York, NY 10031, United States. Tel.: +1 212 650 6641; fax: +1 212 650 7692.
E-mail address: kashfi@med.cuny.edu (K. Kashfi).

0006-2952/$ – see front matter © 2011 Elsevier Inc. All rights reserved.
doi:10.1016/j.bcp.2011.12.019

inflammation and caused significantly less gastric toxicity than diclofenac. It also reduced plasma IL-1β/TNF-α; and elevated plasma IL-10 [15].

NF-κB is a transcription factor that functions in a wide variety of processes from inflammatory reaction and development, to cellular survival and oncogenesis [18]. NF-κB binds to DNA and leads to transcription of genes that contribute to tumorigenesis, such as inflammatory, antiapoptotic genes, and positive regulators of cell proliferation and angiogenesis, and in promoting metastasis in vivo [19,20]. Studies indicate that NF-κB is constitutively activated in estrogen receptor-negative breast cancer cell lines and primary tumors [21–24], and that this event is associated with resistance to apoptosis [25,26], and promotion of an invasive and metastatic phenotype [27]. In several mouse xenograft models, tumor growth is impaired when NF-κB is inhibited [20,28,29]. Therefore, activated NF-κB, constitutes a valid therapeutic target for ER-negative breast cancers and certain subclasses. Changes in the intracellular reduction–oxidation (redox) states have been reported to modulate the activity of NF-κB [30–33].

Many anticancer agents induce reactive oxygen species (ROS) as part of their mechanism of action. A selective state of oxidative stress is generally found in cancer cells, however, a very high ROS level can disrupt redox homeostasis and cause cellular damage, and even induce apoptosis and cell death [34,35]. On the other hand, endogenous redox molecules such as thioredoxins Trxs, which are overexpressed in certain cancers are known to suppresses apoptosis [36]. Trx is a small ubiquitous redox-active thiol protein associated with the enzyme thioredoxin reductase-1 (TrxR) that maintains it in the reduced state [37]. Increased expression of Trx and TrxR is found in several human primary cancers that are associated with aggressive tumor growth including breast carcinoma [38]. Also, there exists some relationships between TrxR inactivation and growth inhibition, cell cycle arrest and apoptosis in colorectal cancer cell lines [39]. Therefore, ROS and Trx/TrxR system are attractive targets for cancer drug development.

In the present study we have demonstrated cell growth inhibition in a triple negative (ER−, PR−, HER−) breast cancer cell line MDA-MB 231, mammary tumor growth inhibition in a xenograft mouse model, and the effect on NF-κB activity by the novel H_2S-releasing compound HS-ASA.

2. Materials and methods

2.1. Reagents and cell culture

HS-aspirin (HS-ASA), [4-(5-thioxo-5H-1, 2-dithiol-3-yl)-phenyl 2-acetoxybenzoate] was synthesized and purified by us with ^{1}H NMR verification as described in the accompanied manuscript. Aspirin and other fine chemicals were obtained from Sigma–Aldrich (St. Louis, MO). Human breast cancer MDA-MB-231 cell line (ER−, PR−, which does not over express Her2) [40] was obtained from the American Type Culture Collection (Manassas,VA) and maintained in Dulbecco's modified Eagle's medium (DMEM) supplemented with 10% heat-inactivated fetal calf serum (FCS), 2 mmol/L L-glutamine and penicillin/streptomycin (100 units/mL), at 37 °C in 5% CO_2 humidified atmosphere. A normal human mammary epithelial (HMEpC) cell line was obtained from Promo Cell, (Heidelberg, Germany) and was cultured in ready-to-use mammary epithelium cell growth medium as suggested by manufacturer.

2.2. MTT assay

Cell growth inhibitory effect of HS-aspirin was measured using a colorimetric MTT assay kit (Roche, Indianapolis, IN). MDA-MB-231 cells were plated overnight in 96-well plates at a density of 30,000 cells/well. The cells were then incubated for 24 h with different concentrations of HS-ASA. After the indicated time, 10 μL of MTT dye (3-[4,5-dimethylthiazol-2-yl]-2,5-diphenyl tetrazolium bromide, 5 mg/mL in phosphate buffered saline), was added to each well, and the plates were incubated for 2 h at 37 °C. This was followed by the addition of 100 μL of the solubilization solution. The absorbance of the plates was measured on an ELISA reader at a wavelength of 570 nm. Each sample was performed in triplicate, and the entire experiment was repeated three times.

2.3. Cell proliferation

PCNA antigen expression was determined using an ELISA Kit (Calbiochem, La Jolla, CA), in accordance with the manufacturers protocol. MDA-MB-231 cells (1×10^6 cells/mL) were incubated with serum-free media for 24 h to remove the effect of endogenous growth factors, they were then treated for 24 h with various concentrations of HS-ASA or vehicle. For the assay, we made a suspension of 1×10^6 cells/mL in suspension buffer (5 mM ethylene diamine tetraacetic acid [EDTA], 0.2 mM PMSF, 1 μg/mL pepstatin, 0.5 μg/mL leupeptin, and 50 mM tris[hydroxymethyl] aminomethane hydrochloride [Tris–HCl] [pH 8.0]). Samples of the suspension were pipetted into the wells of the plate enclosed with the kit, where rabbit polyclonal antibody specific for the human PCNA protein was immobilized. The mouse monoclonal antibody clone PC10 was then added to each well as a detector antibody and the mixture was incubated for 2 h at room temperature. After the wells had been washed, horseradish peroxidase streptavidin was added and the plates were incubated for 30 min at room temperature. The chromogenic substrate tetramethylbenzidine was then added, and the plates were incubated for a further 30 min. Finally, the stop solution was added and the absorbance was measured at 450 nm in a plate reader.

2.4. Cell cycle analysis

Cell cycle phase distributions of control and treated MDA-MB-231 cells were obtained using a Coulter Profile XL equipped with a single argon ion laser. For each subset, >10,000 events were analyzed. All parameters were collected in list mode files. Data were analyzed on a Coulter XL Elite Work station using the Software programs MultigraphTM and MulticycleTM. MDA-MB-231 Cells (0.5×10^6) treated with various concentrations of HS-ASA were fixed in 100% methanol for 10 min at −20 °C, pelleted (5000 rpm × 10 min at 4 °C), resuspended and incubated in PBS containing 1% FBS/0.5% NP-40 on ice for 5 min. Cells were washed again in 500 μL of PBS/1% FBS containing 40 μg/mL propidium iodide (used to stain for DNA) and 200 mg/mL RNase type IIA, and analyzed within 30 min by flow cytometry. The percentage of cells in G_0/G_1, G_2/M, and S phases was determined form DNA content histograms.

2.5. Assay for apoptosis

MDA-MB-231 cells (0.5×10^6 cells/mL) were treated for 24 h with various concentrations of HS-ASA. Cells were washed with and resuspended in 1X Binding Buffer (Annexin V binding buffer, 0.1 M HEPES/NaOH (pH 7.4), 1.4 M NaCl, 25 mM $CaCl_2$; BD BioSciences Pharmingen, San Diego, CA). Then 5 mL of Annexin V-FITC (final concentration 0.5 mg/mL) was added followed by propidium iodide as a counterstain (final concentration 20 mg/mL). The cells were then incubated at room temperature for 15 min in the dark. Finally, the cells were transferred to FACS tubes for analysis. Percentage of apoptotic cells was obtained using a Becton

Dickinson LSR II equipped with a single argon ion laser. For each subset, about 10,000 events were analyzed. All parameters were collected in list mode files. Data was analyzed by Flow Jo software.

2.6. Thioredoxin reductase assay

MDA-MB-231 cells were treated with vehicle or different concentrations of HS-ASA for 24 h, harvested, washed with Dulbecco's phosphate-buffered saline (Invitrogen, Carlsbad, CA) and centrifuged. Cell pellets were resuspended in a hypotonic potassium phosphate buffer (5 mM, pH 7.4, 0.5 mM EDTA), and disrupted by sonication. A post-microsomal supernatant was generated by ultra-centrifugation at 105,000 × *g* for 2 h. The protein concentration of the post-microsomal supernatants was determined by Bradford assay (Bio-Rad Laboratories) with bovine serum albumin as a standard. Thioredoxin reductase activity was measured using a colorimetric assay (Cayman Chemical, Ann Arbor, MI) as described by the manufacturer. Data were collected starting 1 min after the initiation of the reaction to allow non-enzymatic reduction of DTNB [5,5′-dithiobis(2-nitrobenzoic acid)] to go to completion.

2.7. Determination of reactive oxygen species

MDA-MB 231 cells (0.3×10^6 cells/well) were plated in 6-well plates for 24 h after which they were treated with various concentrations of HS-ASA for 1 h. Cells were then trypsinized, washed once in PBS resuspended and then incubated for 30 min at 37 °C in the dark with the oxidation-sensitive fluorescent probes 2′,7′-dichlorodihydrofluorescein diacetate (DCFDA, 10 μM) or dihydroethidium (DHE, 5 μM) (Molecular Probes, Life Technologies, NY). Fluorescence intensity was then measured by flow cytometry using a FACS Calibur (BD Bioscience). DCFDA is a probe for H_2O_2 and other peroxides, while DHE is an intracellular probe that preferentially measures superoxide anion [41,42].

2.8. Nuclear protein extraction and NF-κB p65 transcription factor assay (ELISA) and immunoblotting

MDA-MB-231 cells (2×10^6) were seeded overnight in a 10 cm dish, followed by incubation with various concentrations of HS-ASA for 24 h. Nuclear protein was extracted using a nuclear protein extraction kit (Cayman Chemical Co., Ann Arbor, MI). Protein concentrations were determined with a Bio-Rad reagent (Bio-Rad Laboratories). Nuclear extracts were stored at −80 °C until used. Nuclear extracts were used to detect DNA binding activity of NF-κB by using the NF-κB (p65) transcription factor assay kit (Cayman Chemical) in which the specific DNA sequence containing the NF-κB response element is immobilized in a 96-well plate. Briefly, 50 μg of nuclear proteins were added to the wells with complete transcription factor buffer and incubated overnight in a total volume of 100 μL at 4 °C. Blank wells, positive control (TNF alpha-stimulated HeLa cell nuclear extract provided with kit), and non-specific binding (provided with kit) samples were also included on the plate. NF-κB binding was detected by adding NF-κB primary antibody (except the blank wells) for 1 h at room temperature. A secondary antibody conjugated to HRP was added after washing the wells, and incubated for 1 h at room temperature, followed by addition of 100 μL developing solution, incubation for 45 min with gentle agitation, addition of stop solution, and measurement of absorbance at 450 nm. The reading for nonspecific binding was subtracted from each treatment. The percent change in activity of each test sample relative to the average of untreated samples was determined. For immuno-detection in cell lysates antibodies against IκBα (L35A5), Phospho-IκBα (Ser32) (14D4), NF-κB p65 (D14E12), Phospho-IKKα/β (Ser176/180) (16A6) were obtained from Cell Signaling Technology, (Boston, MA).

2.9. Mouse xenograft model

Male athymic SCID mice, age 5 weeks, were purchased from Charles River Laboratories, Inc., (Wilmington, MA) and were housed according to institutional and NIH guidelines. Human breast cancer MDA-MB-231 cells (5×10^6) suspended in Matrigel (BD Biosciences, San Jose, CA) 50% (v/v) were inoculated subcutaneously in the right flanks of each mouse (six mice per group) using a 1-mL syringe and 22-gauge needles. When the tumors reached an average sizes of ∼60 mm^3, the mice were randomly grouped ($n = 6$) and gavaged daily with either vehicle (1% methylcelloluse) or HS-ASA (100 mg/kg body weight). The tumor size was measured every other day using electronic calipers, the tumor volumes were calculated using the following formula: length × $width^2/2$. Thirty days post inoculation, the mice were sacrificed, the tumors collected, weighed, and photographed. The tumors were stored in formalin for immunohistochemistry studies.

2.10. Immunohistochemistry

All specimens were fixed in formalin and paraffin-enclosed for examination. Five-micrometer-thick tissue sections were prepared to conduct immunohistochemistry. Paraffin-embedded sections were deparaffinized and rehydrated, washed in distilled water, and then subjected to heat mediated antigen retrieval treatment. Endogenous peroxidase activity was quenched by incubation in 2% hydrogen peroxide in methanol for 15 min and then cleared in PBS for 5 min. The sections were blocked for 30 min with 3% normal horse serum diluted in PBS. The sections were then blotted and incubated with primary mouse proliferating cell nuclear antigen, Ki-67 at the appropriate dilution (1:200 dilution) in blocking serum for 4 h at room temperature, or primary rabbit NF-κB p65 antibody (1:100 dilution) in blocking serum overnight at 4 °C. The next day, the slides were washed three times for 5 min each in PBS and incubated with biotinylated anti-rabbit antibody for 2 h. The slides were washed in PBS, followed by formation of the avidinbiotin-peroxidase complex (ABC, Vector Laboratories, Inc.). The slides were washed and the peroxidase reaction was developed with diaminobenzidine and peroxide, then counter-stained with hematoxylin, mounted in para-mount, and evaluated using a light microscope (×200, Carl Zeiss). A negative control was done in all cases by omitting the primary antibody. All slides were counterstained by hematoxylin. For quantification, 200 cells at three randomly selected areas were assessed and the positively proliferating cell nuclear antigen, Ki-67–stained cells were counted and expressed as percentage of stained cells. For NF-κB scoring, for each animal 5 slides were scored by using the following semi-quantitative scoring system as described previously [43]. The *extent of staining* was graded as follows: 0 = no staining; 1+ = ≤25% of cells positive; 2+ = 26–50% of cells positive; 3+ = ≥51% of cells positive. The *intensity of staining* was scored as follows: 0 = no staining; 1+ = faint; 2+ = moderate; 3+ = strong. 1+, 2+ and 3+ were recorded as 1, 2 and 3 points, respectively. To compare differences in staining, an expression index (EI) was calculated by the following formula: EI = extent of staining × intensity of staining. For detection of apoptotic cell death in tumor tissues, the paraffin-embedded sections were then incubated in a mixture of labeling solution (450 μL) and enzyme solution (50 μL) for 1 h at 37 °C and washed three times in 0.1 mol/L PBS for 5 min each according to the manufacturer's instructions (Promega TUNEL System, Madison, WI). The sections were then incubated with diaminobenzidine for 8 min at 37 °C. Finally, the sections were rinsed, mounted on slides, and cover slipped. Positive TUNEL stains were recorded by counting the number of positively stained DAB cells in a defined area.

2.11. Statistical analysis

In vitro data are presented as mean ± SEM for at least three different sets of plates done in triplicate. In vivo treatment groups and number of animals in each group are indicated in the figure legend to Fig. 7. Comparison between treatment groups was performed by one-factor analysis of variance (ANOVA) followed by Tukey's test for multiple comparisons. $P < 0.05$ was regarded as statistically significant.

3. Results

3.1. Cell growth inhibition of MDA MB-231 and HMEpC cells

We evaluated the growth inhibitory effect of HS-ASA using the breast cancer cell line MDA-MB-231. This human cell line is particularly suitable for pre-clinical studies since it is highly aggressive both in vitro and in vivo [44]. Cells that were plated a day earlier were treated with vehicle, or various concentrations of HS-ASA and ASA for 24 h, growth inhibition was measured using the MTT assay, and IC_{50} values were determined. HS-ASA inhibited the growth of MDA-MB-231 cells in a concentration-dependent manner; the IC_{50} of HS-ASA was 3.6 ± 0.5 μM (Fig. 1). In contrast, conventional ASA at 24 h, in concentrations up to 5 mM failed to inhibit the growth of the cells by 50% or more, which is in agreement with previous findings in several types of cancer cells [45–47]. This represents a >1000-fold increase in the potency of HS-ASA. We next evaluated the effects of HS-ASA on a normal human mammary epithelial cell line HMEpC. After 24 h treatment with 10 μM HS-ASA, only 28% of MDA MB-231 remained viable. However, under the same experimental conditions, 78% of HMEpC cells were viable (Fig. 2). The IC_{50}s for cell growth inhibition were 3.5 ± 0.4 and 27.2 ± 0.8 μM for the MDA MB-231 and HMEpC cells, respectively at 24 h. This indicates that HS-ASA inhibits cell growth preferentially in breast cancer cells compared with normal epithelial mammary cell line.

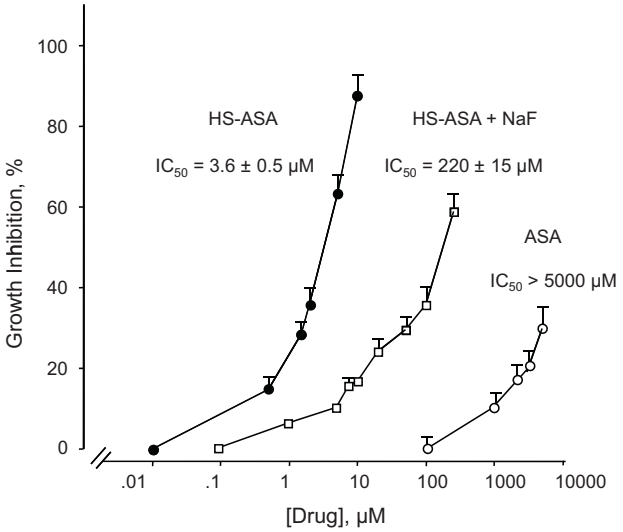

Fig. 1. Inhibitory effect HS-ASA on MDA-MB-231 cell growth. Cells were incubated with increasing concentrations of the HS-ASA or ASA for 24 h. Cell viability was determined by MTT assay as described in Section 2. In some experiments the cells were pre-treated for 6 h with 15 μM NaF a carboxylesterase enzyme inhibitor before HS-ASA treatment. NaF partially reverses HS-ASA mediated cell growth inhibition. Results represent mean ± SEM of at least three different experiments with duplicate plates.

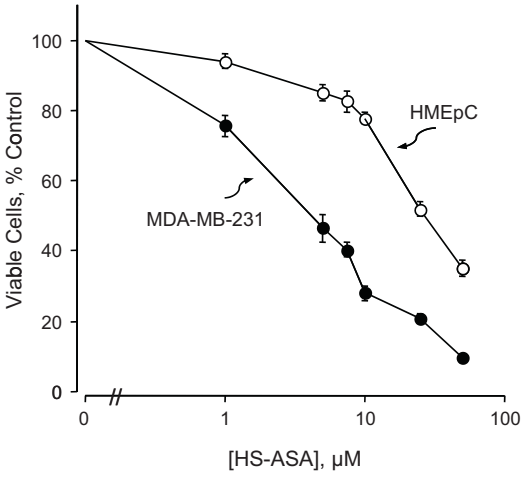

Fig. 2. Differential cytotoxic effect of HS-ASA in breast cancer cell line MDA-MB-231 compared with the normal human mammary epithelial cell line HMEpC. Cells were incubated without or with variable concentrations of HS-ASA for 24 h. Cell viability was determined by MTT assay as described in Section 2. Results are mean ± SEM of three different experiments with duplicate plates.

3.2. Effect of HS-HSA on proliferation, cell cycle progression, and apoptosis

To investigate the effect of HS-ASA on proliferation, MDA-MB-231 cells were treated with HS-ASA at actual (1×, or 3.6 μM), half (0.5×, or 1.8 μM) or twice (2×, or 7.2 μM) the IC_{50} concentration for 24 h, followed by determination of PCNA antigen expression. HS-ASA reduced PCNA expression in these cells in a dose dependent manner up to the highest dose studied; thus at 0.5×, 1×, and 2× IC_{50} the reduction was 21 ± 2%, 53 ± 3% and 64 ± 2%, respectively (Fig. 3A). HS-ASA also affected the cell cycle progression as measured by DNA content of treated-MDA-MB-231 cells using flow cytometry. Cells treated with 0.5×, 1×, and 2× IC_{50} HS-ASA accumulated progressively in G_0/G_1 phase (Fig. 3B). For example, at 1× IC_{50} the cell populations in the different phases were altered as follows compared to control: G_0/G_1 increased from 41.9 ± 2% to 64.3 ± 1.7%; S phase was reduced from 34.8 ± 3.3% to 14.6 ± 3.3%, and G_2/M reduced appreciably from 23.3 ± 2.2% to 12.7 ± 3.2%. An arrest at G_0/G_1 phase was evident at 1× and 2× IC_{50} HS-ASA compared to control; G_0/G_1 increased to 64.3 ± 1.7% and 76.1 ± 2.3%, respectively, while the population in S phase was reduced to 23 ± 1.7 and 14.6 ± 1.2%, and G_2/M was reduced to 12.7 ± 1.2% and 9.3 ± 2.2%, respectively. Finally, the proportion of cells in apoptosis increased in a dose dependent manner as estimated by the Annexin V-FITC staining and flow cytometry. Treatment with 0.5×, 1× and 2× IC_{50} HS-ASA resulted in 15 ± 2%, 43 ± 3%, and 64 ± 5% cells in early apoptotic phase, respectively, compared to untreated control (Fig. 3C). Therefore, HS-ASA inhibits proliferation of MDA-MB-231 cells by a combined induction of G_0/G_1 arrest and apoptosis.

3.3. H_2S release is required for effect of HS-ASA

Published work by others has shown that HS-NSAIDs release H_2S [15,48–50]. In order for H_2S to be released from HS-ASA the ester bond linking the ADT-OH moiety to the ASA molecules has to be hydrolysed. Therefore, we used NaF, a carboxylesterase enzyme inhibitor [15], and examined if HS-ASA-mediated H_2S release was necessary for the cell growth inhibitory effect in MDA-MB-231 cells. Cells were treated with increasing concentration of HS-ASA without or with 15 μM NaF, followed by cell growth determination by MTT assay. Fig. 1 shows that inhibition of H_2S release by NaF strongly reversed HS-ASA mediated cell growth inhibition, although not completely. The IC_{50} for the combination increased to 220 ± 15 μM, which is approximately 60 times less potent than HS-ASA, thus, demonstrating that H_2S release is necessary, in part, for cell growth inhibition by HS-ASA.

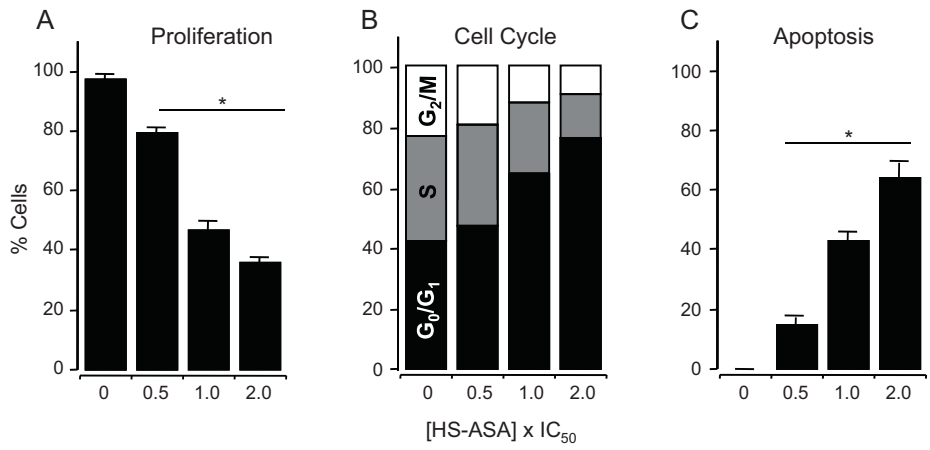

Fig. 3. HS-ASA inhibits proliferation by altering cell cycle progression and inducing apoptosis. Cells were treated with vehicle, 0.5× IC_{50} (1.8 μM), 1× IC_{50} (3.6 μM) or 2× IC_{50} (7.2 μM) HS-ASA for 24 h and analyzed for (A) proliferation by PCNA antigen expression; (B) cell cycle phases by PI staining and flow cytometry; (C) apoptosis by Annexin V staining and flow cytometry. In (A) and (C), results are mean ± SEM for 3 different experiments performed in duplicate, $^*P < 0.05$ compared to control. In (B), results are representative of two different experiments. This study was repeated twice generating results within 10% of those presented here.

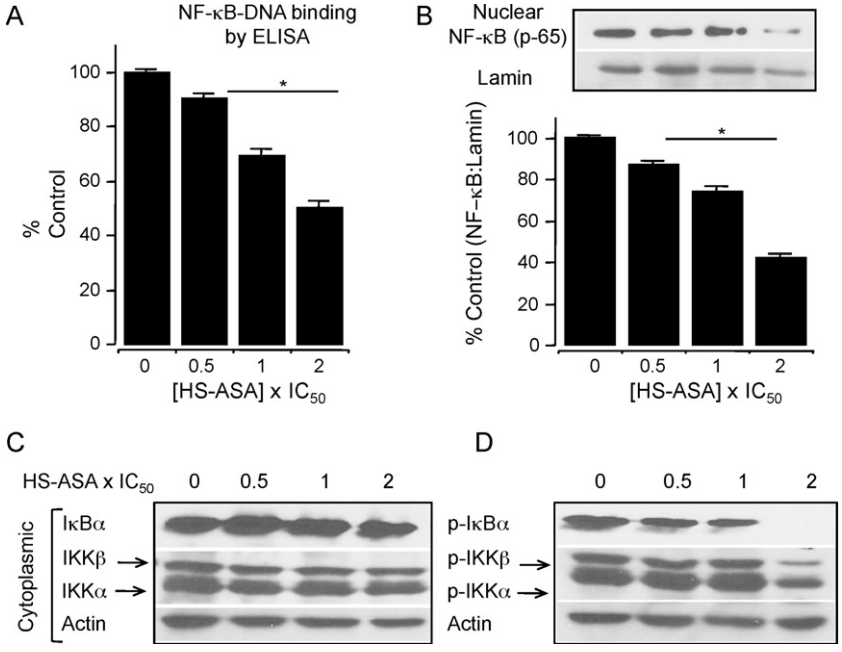

Fig. 4. HS-ASA inhibited NF-κB transcription factor activity in MDA-MB-231 cells. (A) Cells were treated with vehicle or HS-ASA for 24 h and nuclear proteins were harvested. DNA binding activity of NF-κB was determined from nuclear extracts by ELISA for each sample relative to the vehicle control (100%). (B) Nuclear protein extracts was examined for levels of p65 subunit of NF-κB by immunoblotting. (C) Cytoplasmic fractions of HS-ASA-treated cells were examined for total IκBα, IKKα and IKKβ levels, and (D) for phosphorylated IκBα, −IKKα and −IKKβ by immunoblotting. Results are mean ± SEM of 3 different sets of experiments. $^*P < 0.05$ compared to vehicle treated controls.

3.4. HS-ASA inhibits NF-κB DNA binding and thioredoxin reductase activity

Since NF-κB is implicated in cell survival and oncogenesis, we examined NF-κB activity during HS-ASA-mediated cell growth response. Nuclear extracts from HS-ASA treated cells were examined as described in Section 2. HS-ASA significantly inhibited DNA binding activity of NF-κB (p65) in a concentration dependent manner in MDA-MB 231cells, at 6 h (Fig. 4A). HS-ASA at concentrations equivalent to 1× IC_{50} and 2× IC_{50} reduced the NF-κB-DNA binding activity to approximately 71% and 50%, respectively. Therefore the reduction in DNA binding was substantial only at twice the IC_{50} concentration. We measured the level of nuclear p65, the functionally active subunit of NF-κB, HS-ASA, at 1× and 2× IC_{50} concentrations reduced nuclear p65 levels to approximately 78% and 66%, respectively (Fig. 4B). The decrease in DNA binding activity was associated with decrease in NF-κB protein p65 levels in the nucleus. One of the most critical steps in NF-κB activation is its dissociation from IκB, which is mediated through phosphorylation and subsequent proteolytic degradation of this inhibitory subunit [51,52]. To determine whether the inhibitory effect of HS-ASA on NF-κB DNA binding was due to reduced translocation of p65 into the nucleus by suppression of IκBα degradation via phosphorylation, we determined the phosphorylation status of IκBα in the cytoplasm. HS-ASA decreased phospho-IκBα levels and higher concentration of HS-ASA completely inhibited IκBα phosphorylation while total levels were unaltered (Fig. 4C and D). Thus, HS-ASA inhibits

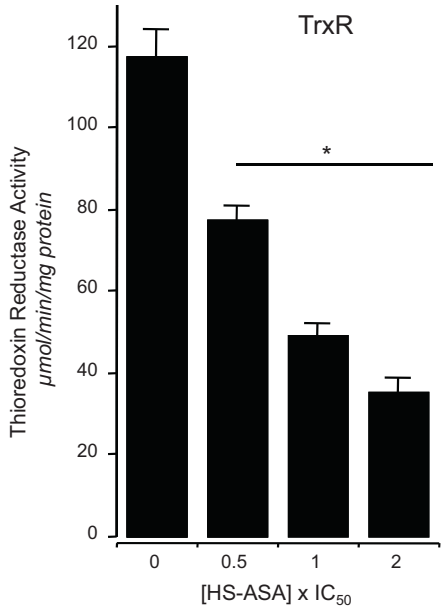

Fig. 5. Thioredoxin reductase activity is reduced by HS-ASA. Cells were treated with vehicle or 0.5×, 1×, and 2× IC_{50} HS-ASA for 24 h, followed by measurement of thioredoxin reductase activity (μmol/min/mg) as described in Section 2. TrxR activity was reduced by HS-ASA in a dose-dependent manner. Results are mean ± SEM of 3 different experiments performed in duplicate. *$P < 0.02$ compared to vehicle treated controls.

translocation of p65 to the nucleus through blockade of IκBα phosphorylation. The phosphorylation of the IκBs are known to be mediated by IkappaKinases (IKKs) namely IKKα and IKKβ, which are activated by phosphorylation at specific serine residues in the activation loop of IKKβ [51]. HS-ASA decreased the phosphorylation of both IKKα and IKKβ without affecting total IKK levels (Fig. 4C and D). Therefore, HS-ASA prevents activation of IKKs, inhibits phosphorylation-mediated degradation of IκBα, and prevents translocation of NF-κB-p65 into the nucleus. This effect was more prominent at 2× IC_{50} values.

The redox balance of the cells may influence the function of NF-κB by regulating its ability to bind to DNA [30,31,53,54]. We examined thioredoxin reductase activity in MDA-MB 231 breast cancer cells in response to various concentrations of HS-ASA. There was a strong inhibition of TrxR activity; 0.5×, 1× and 2× IC_{50} HS-ASA reduced the activity of TrxR to 78%, 51% and 38%, respectively, compared to control (Fig. 5).

3.5. HS-ASA induces ROS

We examined whether HS-ASA induced ROS levels. DCFDA is a molecular probe that detects greater than ten individual reactive species [55,56]. Cells were treated with different concentrations of HS-ASA for 1 h, stained with DCFDA, and analyzed for levels of intracellular peroxides. Compared with control, increasing concentrations of HS-ASA increased the population of cells showing DCFDA-dependent fluorescence, indicating an induction of intracellular peroxides (Fig. 6A and B). ROS increased to 15-fold by 1× IC_{50} HS-ASA, followed by a marked increase to 47-fold by 2× IC_{50} HS-ASA, compared with basal levels. We also monitored intracellular levels of superoxide anion ($O_2^{\bullet -}$) generated by HS-ASA using dihydroethidium (DHE), a selective probe for $O_2^{\bullet -}$ [57]. HS-ASA clearly increased $O_2^{\bullet -}$ levels (Fig. 6C and D), confirming ROS generation. The increase in superoxide anions levels was evident at 0.5× IC_{50}, which increased markedly at 1× IC_{50} that was followed by a reduction at 2× IC_{50}.

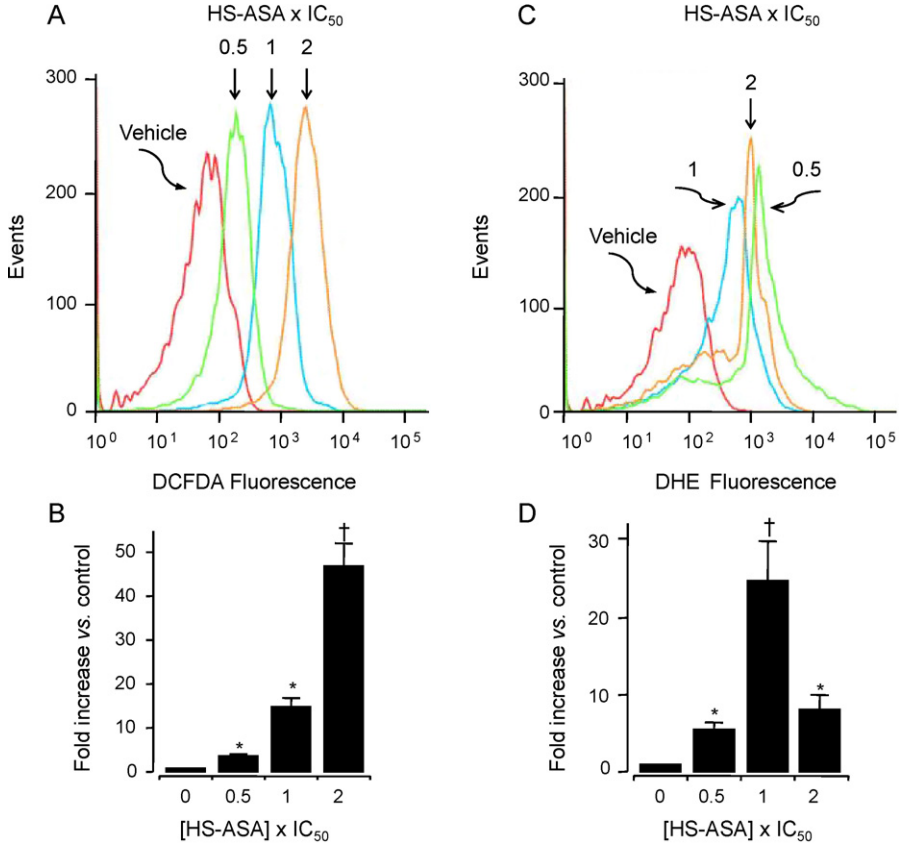

Fig. 6. HS-ASA induces ROS levels. MDA-MB-231 cells were treated with HS-ASA for 1 h followed by staining with a general ROS probe DCFDA (A) or DHE which detects superoxide anions in cells (B). A representative histograms are shown. Values are the mean ± SEM of three independent experiments. *$P < 0.05$ compared to untreated controls.

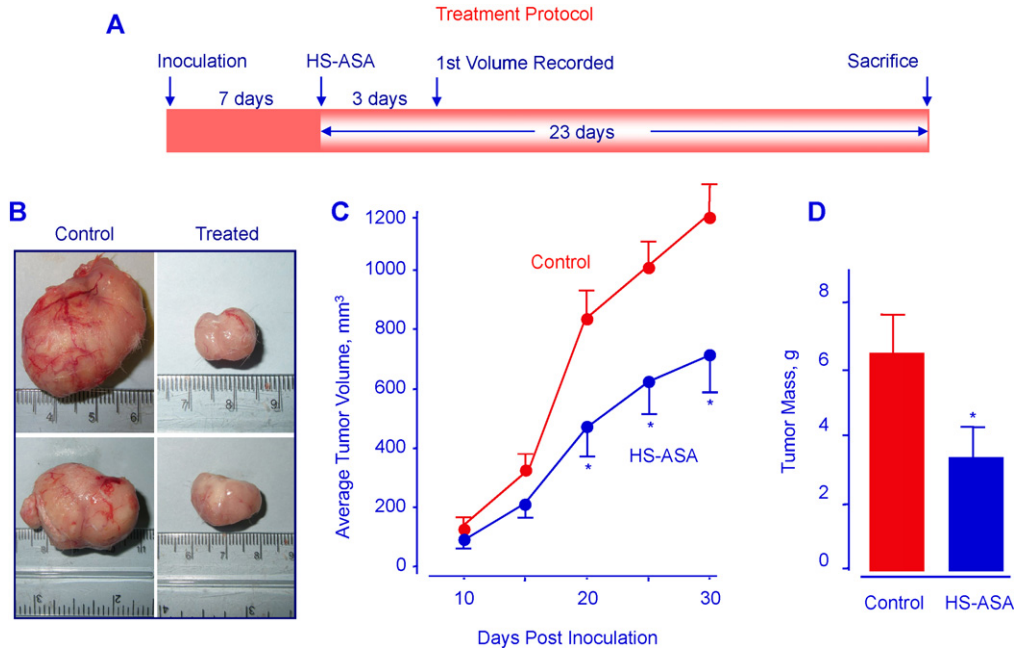

Fig. 7. HS-ASA inhibits tumor xenograft growth. Athymic SCID male mice were injected subcutaneously with MDA-MB-231 cells for the development of subcutaneous tumors as described in Section 2. Following tumor formation, the mice were randomly divided into 2 groups ($N = 6$) and treated daily with vehicle or 100 mg/kg HS-ASA for 23 days according to the protocol in panel A. Representative tumor sizes for untreated and treated mice are shown in panel B. Average tumor volume as function of time and tumor mass at sacrifice are shown in panels C and D, respectively. HS-ASA significantly reduced tumor volume from day 20 post inoculation to sacrifice, $P < 0.05$. Tumor mass was also significantly reduced by HS-ASA treatment, $P < 0.05$.

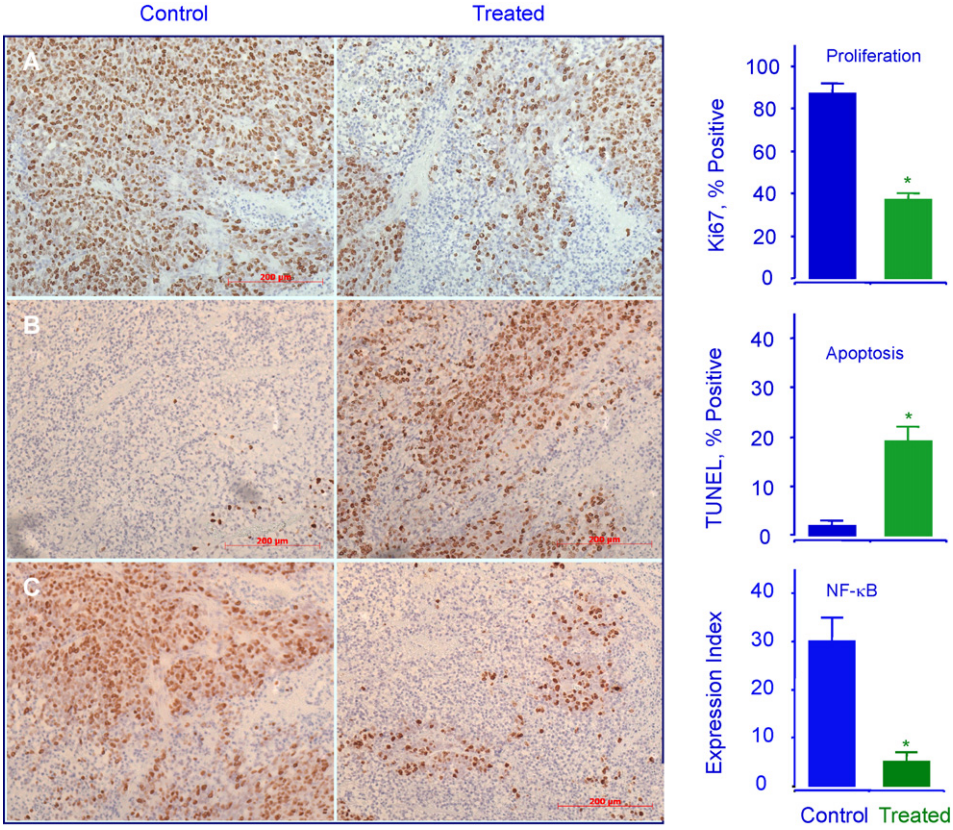

Fig. 8. HS-ASA inhibits proliferation, induces apoptosis and decreases NF-κB p65 in vivo. Stored tumors were sectioned, probed, and scored as described in Section 2. Average mitotic index at sacrifice was determined by Ki-67 staining ($P < 0.05$), TUNEL staining ($P < 0.02$) and p65 staining ($P < 0.02$). Representative fields used for quantification of the staining are shown. The scale bar represents 200 μm.

3.6. Effect of HS-ASA on tumor growth in a xenograft model

Athymic SCID male mice were injected subcutaneously with MDA-MB-231cells in the right flank, allowing for the development of subcutaneous tumors after 7 days. Using male mice was a distinct feature in our study to focus specifically on HS-ASA-induced changes without estrogen interference, since estrogen has diverse effects on tumor phenotype of tumors and on angiogenesis [58]. MDA-MB-231 is an estrogen-independent cell line that does not require exogenously added estrogen for xenograft growth, and is ideally suited for TNBC studies. Following tumor formation, six mice were treated everyday for 23 days with 100 mg/kg HS-ASA, whereas six control mice were left untreated for the same period of time. At the end of the study, HS-ASA-treated mice showed a considerable reduction in tumor volume compared with untreated mice (Fig. 7). Compared with the control group with mean tumor volume of $1269 \pm 110\ mm^3$, HS-ASA reduced the tumor volume to $712 \pm 118\ mm^3$, equivalent to a mean reduction of 44% ($P < 0.05$). Compared to the control group with average tumor mass 6.4 ± 1.1 g, HS-ASA reduced the tumor mass to 3.4 ± 0.8 g, equivalent to a reduction of 47% ($P < 0.05$), which was consistent with continued regression of tumor volume over the same treatment period.

The primary endpoint of tumor cell proliferation (mitotic index) was assessed by Ki67, a biomarker of proliferation which is a highly prognostic factor in breast cancer [59]. Immunohistochemical expression of HS-ASA-treated and untreated mouse tumor sections was evaluated for Ki-67 and NF-κB p65. The untreated tumors showed a strong expression index of Ki67 and NF-κB (Fig. 8A and C, control panel), whereas HS-ASA-treated tumors showed a diminished expression of NF-κB and Ki67 (Fig. 8A and C, treated panel). HS-ASA treatment was also accompanied with increased number of cells undergoing apoptotic death (20%) compared with control (1.5%) (Fig. 8B).

4. Discussion

In the present study, HS-ASA exhibited anti-breast cancer activity both in vitro and in vivo. HS-ASA induced apoptosis and inhibited cell proliferation in chemoresistant ER-negative breast cancer cells, and reduced mammary tumor growth in a mouse xenograft model.

HS-ASA appears to recruit several cellular events to inhibit cellular growth as suggested by our in vitro studies. The growth inhibitory effect of HS-ASA is associated with G_1 to S cell cycle arrest, inhibition of proliferation and induction of apoptosis. Low concentration of HS-ASA, such as $1\times$ IC_{50}, significantly reduced the proportion of cells in S phase and blocked DNA synthesis inhibiting cell renewal, whereas higher concentration of HS-ASA ($2\times$ IC_{50}) induced cell death in a large population (64%) of the cells. Thus, the proapoptotic effect of HS-ASA suggests strong antineoplastic potential. Strong antiproliferative effects of H_2S, by endogenous overproduction or exogenous addition have been reported in HEK293 embryonic kidney cells [60], while decreased cell viability was reported at physiological concentration of H_2S in a WiDr cancer cell line of colon origin [61]. However, apoptotic response of endogenous H_2S is known to vary depending on tissue type. For example, a pro-apoptotic response occurs on aorta smooth muscle cells [60] whereas cytoprotection occurs in endothelial cells [62,63]. Consistent with our studies in cancer cells, an H_2S releasing compound GYY4137 induced apoptosis and cell cycle arrest in several human cancer cell lines, including the ER positive MCF-7 cells [50]. However, this compound is not NSAID based and therefore lacks any potential advantages that an H_2S-releasing NSAID may have.

Encouraged by our findings in the ER-cells, we examined the effects of HS-ASA treatment in a mouse xenograft model. Tumor xenografts representing human estrogen-responsive negative breast cancer underwent large reductions in volume and mass. Decrease in tumor size and mass was associated with inhibition of cell proliferation and induction of apoptosis. The dose of HS-ASA in this mouse model appeared to be well tolerated with no apparent harmful side-effects or overall gross toxicity observed. Our study adds to the repertoire of a number of independent studies that have demonstrated beneficial effects of H_2S or sulfide-donor compounds in animal models of disease and cancer [17,48,50,64–69].

In this study, the plausible event is that HS-ASA was utilized enzymatically by MDA-MB-231 cells, releasing H_2S. This is based on the observation that NaF, a known inhibitor carboxylesterase enzyme activity, reversed HS-ASA-facilitated cell growth inhibition. Although spontaneous release of H_2S following incubation in a culture medium may also be expected, and probably does occur, the fact that NaF strongly reversed cell growth inhibition suggests that spontaneous H_2S generation by HS-ASA is either low or slow.

At the level of biochemical events, some known molecular targets of H_2S are intracellular signaling proteins and transcription factors. The interaction of H_2S with transcription factors has received much attention in recent studies particularly with respect to its role in inflammation and tissue ischemia [70]. Since certain classes of ER negative breast cancers depend on NF-κB for proliferation [71], our finding that HS-ASA inhibits NF-κB signaling mediated by blockade of IκBα phosphorylation by inhibiting IKK activity, is significant, although this occurred strongly at $2\times$ IC_{50} concentration. Similar inhibition of IKK/NF-κB signaling occurred by H_2S-releasing diclofenac in osteoclasts and by the cancer preventive compound curcumin in Jurkat T cells [72,73]. In our study, it is encouraging that this inhibition of NF-κB was associated with a decreased mitotic index (suppression of Ki67) in the tumors of the HS-ASA treated animals

Since cellular redox mechanisms may be affected by H_2S we examined the Trx/TrxR system, which are required for the maintenance of essential cysteine residues in the active thiol forms in certain proteins including the NF-κB protein [31]. Trxs are also overexpressed in certain cancers and are known to suppresses apoptosis [36]. Here it was an interesting finding that HS-ASA moderately inhibited the activity of TrxR enzyme, the inhibition being 50% at its IC_{50}. Also, as noted above, at its IC_{50} concentration, HS-ASA led to a moderate inhibition of NF-κB-activity through inhibition of IKK activation. However, in light of a recent report describing that TrxR activity does not affect cytoplasmic activation, nuclear translocation, or DNA-binding activity of NF-κB [74], we believe that inactivation of TrxR may be important through a combined effect with ROS. Overall, since molecular targets in ER-breast cancer are few and are a major therapeutic issue, the breast cancers that rely on NF-κB activation for aberrant cell proliferation are appropriate candidates for examination of response to HS-ASA.

Nitric oxide-releasing aspirin has also been shown to exert apoptotic effects on cancer cells via ROS generation [75,76]. Oxidative stress is produced in cells when there is disturbance in the equilibrium between ROS formation and endogenous antioxidant defense mechanisms. It is well accepted that cancer cells have high constitutive oxidative stress levels [77] and may be pushed over a threshold to cell death by exogenous ROS. In our study, HS-ASA induced cell cycle changes and apoptosis in MDA-MB-231 cells, which was associated with parallel increase in ROS levels and decrease in Trx reductase activity, both of which appear to favor cell death. Interestingly, increases in the ROS superoxide anion levels dropped markedly at $2\times$ IC_{50} HS-ASA, (Fig. 6C and D), even though a larger number of cells were apoptotic (64%). Since the molecular mechanisms of the oxidative responses are not completely understood, this remains unclear. Increase in oxidative stress appears to be an early event as ROS levels are induced at

early time point of 1 h at low concentration of half the IC_{50} value. It has been reported that inhibition of the NF-κB signaling pathway resulted in induction of massive oxidative stress and cell death in cutaneous T-cell lymphoma cell lines [78]. Therefore, a collective effect of ROS induction and inhibition of the NF-κB likely contribute to HS-ASA's overall mechanism of action.

In conclusion, HS-ASA, suppressed the growth MDA-MB-231 cells by induction of apoptosis and alteration of cell cycle phases. This effect correlated with down-regulation of NF-κB activity,TrxR activity, and induction of ROS. Therefore, HS-ASA demonstrates therapeutic potential in ER-breast cancer treatment and warrants further study.

Acknowledgment

Supported in part by the National Cancer Institute through a subcontract from ThermoFisher, contract # FBS-43312-26.

References

[1] Wood WC, Muss HB, Solin LJ, Olopade OI. Malignant tumors of the breast. In: DeVita VT, Hellman S, Rosenberg SA, editors. Cancer: principles and practice of oncology. Philadelphia: Lippincott-Raven; 2005. p. 1415–77.
[2] Jemal A, Bray F, Center MM, Ferlay J, Ward E, Forman D. Global cancer statistics. CA Cancer J Clin 2011;61:69–90.
[3] Osborne CK. Tamoxifen in the treatment of breast cancer. N Engl J Med 1998;339:1609–18.
[4] Sheikh MS, Garcia M, Pujol P, Fontana JA, Rochefort H. Why are estrogen-receptor-negative breast cancers more aggressive than the estrogen-receptor-positive breast cancers? Invasion Metastasis 1994;14:329–36.
[5] Carey LA, Dees EC, Sawyer L, Gatti L, Moore DT, Collichio F, et al. The triple negative paradox: primary tumor chemosensitivity of breast cancer subtypes. Clin Cancer Res 2007;13:2329–34.
[6] Fisher DE. Apoptosis in cancer therapy: crossing the threshold. Cell 1994;78: 539–42.
[7] Kaufmann SH. Induction of endonucleolytic DNA cleavage in human acute myelogenous leukemia cells by etoposide, camptothecin, and other cytotoxic anticancer drugs: a cautionary note. Cancer Res 1989;49:5870–8.
[8] Hinz B, Brune K. Cyclooxygenase-2—10 years later. J Pharmacol Exp Ther 2002;300:367–75.
[9] Umar A, Viner JL, Anderson WF, Hawk ET. Development of COX inhibitors in cancer prevention and therapy. Am J Clin Oncol 2003;26:S48–57.
[10] Joki T, Heese O, Nikas DC, Bello L, Zhang J, Kraeft SK, et al. Expression of cyclooxygenase 2 (COX-2) in human glioma and in vitro inhibition by a specific COX-2 inhibitor, NS-398. Cancer Res 2000;60:4926–31.
[11] Cao Y, Pearman AT, Zimmerman GA, McIntyre TM, Prescott SM. Intracellular unesterified arachidonic acid signals apoptosis. Proc Natl Acad Sci USA 2000;97: 11280–5.
[12] Tsujii M, Kawano S, Tsuji S, Sawaoka H, Hori M, DuBois RN. Cyclooxygenase regulates angiogenesis induced by colon cancer cells. Cell 1998;93:705–16.
[13] Wallace JL. How do NSAIDs cause ulcer disease? Baillieres Best Pract Res Clin Gastroenterol 2000;14:147–59.
[14] Li L, Bhatia M, Moore PK. Hydrogen sulphide—a novel mediator of inflammation. Curr Opin Pharmacol 2006;6:125–9.
[15] Li L, Rossoni G, Sparatore A, Lee LC, Del Soldato P, Moore PK. Anti-inflammatory and gastrointestinal effects of a novel diclofenac derivative. Free Radic Biol Med 2007;42:706–19.
[16] Wang R. Two's company, three's a crowd: can H_2S be the third endogenous gaseous transmitter. FASEB J 2002;16:1792–8.
[17] Distrutti E, Sediari L, Mencarelli A, Renga B, Orlandi S, Russo G, et al. 5-Amino-2-hydroxybenzoic acid 4-(5-thioxo-5H-[1,2]dithiol-3yl)-phenyl ester (ATB-429), a hydrogen sulfide-releasing derivative of mesalamine, exerts antinociceptive effects in a model of postinflammatory hypersensitivity. J Pharmacol Exp Ther 2006;319:447–58.
[18] Chen F, Castranova V, Shi X. New insights into the role of nuclear factor-kappaB in cell growth regulation. Am J Pathol 2001;159:387–97.
[19] Luo JL, Kamata H, Karin M. IKK/NF-kappaB signaling: balancing life and death—a new approach to cancer therapy. J Clin Invest 2005;115:2625–32.
[20] Karin M, Cao Y, Greten FR, Li ZW. NF-kappaB in cancer: from innocent bystander to major culprit. Nat Rev Cancer 2002;2:301–10.
[21] Nakshatri H, Bhat-Nakshatri P, Martin DA, Goulet Jr RJ, Sledge Jr GW. Constitutive activation of NF-kappaB during progression of breast cancer to hormone-independent growth. Mol Cell Biol 1997;17:3629–39.
[22] Sovak MA, Bellas RE, Kim DW, Zanieski GJ, Rogers AE, Traish AM, et al. Aberrant nuclear factor-kappaB/Rel expression and the pathogenesis of breast cancer. J Clin Invest 1997;100:2952–60.
[23] Biswas DK, Cruz AP, Gansberger E, Pardee AB. Epidermal growth factor-induced nuclear factor kappa B activation: a major pathway of cell-cycle progression in estrogen-receptor negative breast cancer cells. Proc Natl Acad Sci USA 2000;97:8542–7.
[24] Romieu-Mourez R, Landesman-Bollag E, Seldin DC, Traish AM, Mercurio F, Sonenshein GE. Roles of IKK kinases and protein kinase CK2 in activation of nuclear factor-kappaB in breast cancer. Cancer Res 2001;61:3810–8.
[25] Patel NM, Nozaki S, Shortle NH, Bhat-Nakshatri P, Newton TR, Rice S, et al. Paclitaxel sensitivity of breast cancer cells with constitutively active NF-kappaB is enhanced by IkappaBalpha super-repressor and parthenolide. Oncogene 2000;19:4159–69.
[26] Weldon CB, Burow ME, Rolfe KW, Clayton JL, Jaffe BM, Beckman BS. NF-kappa B-mediated chemoresistance in breast cancer cells. Surgery 2001;130:143–50.
[27] Nakshatri H, Goulet Jr RJ. NF-kappaB and breast cancer. Curr Probl Cancer 2002;26:282–309.
[28] Reuther JY, Reuther GW, Cortez D, Pendergast AM, Baldwin Jr AS. A requirement for NF-kappaB activation in Bcr-Abl-mediated transformation. Genes Dev 1998;12:968–81.
[29] Baldwin AS. Control of oncogenesis and cancer therapy resistance by the transcription factor NF-kappaB. J Clin Invest 2001;107:241–6.
[30] Ueno M, Masutani H, Arai RJ, Yamauchi A, Hirota K, Sakai T, et al. Thioredoxin-dependent redox regulation of p53-mediated p21 activation. J Biol Chem 1999;274:35809–15.
[31] Matthews JR, Wakasugi N, Virelizier JL, Yodoi J, Hay RT. Thioredoxin regulates the DNA binding activity of NF-kappa B by reduction of a disulphide bond involving cysteine 62. Nucleic Acids Res 1992;20:3821–30.
[32] Muller JM, Rupec RA, Baeuerle PA. Study of gene regulation by NF-kappa B and AP-1 in response to reactive oxygen intermediates. Methods 1997;11:301–12.
[33] Powis G, Montfort WR. Properties and biological activities of thioredoxins. Annu Rev Biophys Biomol Struct 2001;30:421–55.
[34] Dalle-Donne I, Giustarini D, Colombo R, Rossi R, Milzani A. Protein carbonylation in human diseases. Trends Mol Med 2003;9:169–76.
[35] Circu ML, Aw TY. Reactive oxygen species, cellular redox systems, and apoptosis. Free Radic Biol Med 2010;48:749–62.
[36] Arner ES, Holmgren A. The thioredoxin system in cancer. Semin Cancer Biol 2006;16:420–6.
[37] Mustacich D, Powis G. Thioredoxin reductase. Biochem J 2000;346(Pt 1):1–8.
[38] Lincoln DT, Ali Emadi EM, Tonissen KF, Clarke FM. The thioredoxin-thioredoxin reductase system: over-expression in human cancer. Anticancer Res 2003;23:2425–33.
[39] Zhao F, Yan J, Deng S, Lan L, He F, Kuang B, et al. A thioredoxin reductase inhibitor induces growth inhibition and apoptosis in five cultured human carcinoma cell lines. Cancer Lett 2006;236:46–53.
[40] Subik K, Lee JF, Baxter L, Strzepek T, Costello D, Crowley P, et al. The Expression Patterns of ER, PR, HER2, CK5/6, EGFR, Ki-67 and AR by Immunohistochemical Analysis in Breast Cancer Cell Lines. Breast Cancer (Auckl) 2010;4:35–41.
[41] Sundaresan M, Yu ZX, Ferrans VJ, Irani K, Finkel T. Requirement for generation of H_2O_2 for platelet-derived growth factor signal transduction. Science 1995;270:296–9.
[42] Robinson KM, Janes MS, Pehar M, Monette JS, Ross MF, Hagen TM, et al. Selective fluorescent imaging of superoxide in vivo using ethidium-based probes. Proc Natl Acad Sci USA 2006;103:15038–43.
[43] Ouyang N, Williams JL, Tsioulias GJ, Gao J, Iatropoulos MJ, Kopelovich L, et al. Nitric oxide-donating aspirin prevents pancreatic cancer in a hamster tumor model. Cancer Res 2006;66:4503–11.
[44] Price JE, Polyzos A, Zhang RD, Daniels LM. Tumorigenicity and metastasis of human breast carcinoma cell lines in nude mice. Cancer Res 1990;50:717–21.
[45] Kashfi K, Ryan Y, Qiao LL, Williams JL, Chen J, Del Soldato P, et al. Nitric oxide-donating nonsteroidal anti-inflammatory drugs inhibit the growth of various cultured human cancer cells: evidence of a tissue type-independent effect. J Pharmacol Exp Ther 2002;303:1273–82.
[46] Kashfi K, Borgo S, Williams JL, Chen J, Gao J, Glekas A, et al. Positional isomerism markedly affects the growth inhibition of colon cancer cells by nitric oxide-donating aspirin in vitro and in vivo. J Pharmacol Exp Ther 2005;312:978–88.
[47] Nath N, Vassell R, Chattopadhyay M, Kogan M, Kashfi K. Nitro-aspirin inhibits MCF-7 breast cancer cell growth: effects on COX-2 expression and Wnt/beta-catenin/TCF-4 signaling. Biochem Pharmacol 2009;78:1298–304.
[48] Li L, Bhatia M, Zhu YZ, Zhu YC, Ramnath RD, Wang ZJ, et al. Hydrogen sulfide is a novel mediator of lipopolysaccharide-induced inflammation in the mouse. FASEB J 2005;19:1196–8.
[49] Huang S, Chua JH, Yew WS, Sivaraman J, Moore PK, Tan CH, et al. Site-directed mutagenesis on human cystathionine-gamma-lyase reveals insights into the modulation of H_2S production. J Mol Biol 2010;396:708–18.
[50] Lee ZW, Zhou J, Chen CS, Zhao Y, Tan CH, Li L, et al. The slow-releasing hydrogen sulfide donor, GYY4137, exhibits novel anti-cancer effects in vitro and in vivo. PLoS One 2011;6:e21077.
[51] Bonizzi G, Karin M. The two NF-kappaB activation pathways and their role in innate and adaptive immunity. Trends Immunol 2004;25:280–8.
[52] Ghosh S, Karin M. Missing pieces in the NF-kappaB puzzle. Cell 2002;109 (Suppl.):S81–96.
[53] Bannister AJ, Cook A, Kouzarides T. In vitro DNA binding activity of Fos/Jun and BZLF1 but not C/EBP is affected by redox changes. Oncogene 1991;6: 1243–50.
[54] Cromlish JA, Roeder RG. Human transcription factor IIIC (TFIIIC). Purification, polypeptide structure, and the involvement of thiol groups in specific DNA binding. J Biol Chem 1989;264:18100–9.
[55] Bass DA, Parce JW, Dechatelet LR, Szejda P, Seeds MC, Thomas M. Flow cytometric studies of oxidative product formation by neutrophils: a graded response to membrane stimulation. J Immunol 1983;130:1910–7.

[56] LeBel CP, Ischiropoulos H, Bondy SC. Evaluation of the probe 2′,7′-dichlorofluorescin as an indicator of reactive oxygen species formation and oxidative stress. Chem Res Toxicol 1992;5:227–31.
[57] Becker LB, vanden Hoek TL, Shao ZH, Li CQ, Schumacker PT. Generation of superoxide in cardiomyocytes during ischemia before reperfusion. Am J Physiol 1999;277:H2240–6.
[58] Hyder SM, Stancel GM. Regulation of angiogenic growth factors in the female reproductive tract by estrogens and progestins. Mol Endocrinol 1999;13:806–11.
[59] Urruticoechea A, Smith IE, Dowsett M. Proliferation marker Ki-67 in early breast cancer. J Clin Oncol 2005;23:7212–20.
[60] Yang G, Cao K, Wu L, Wang R. Cystathionine gamma-lyase overexpression inhibits cell proliferation via a H_2S-dependent modulation of ERK1/2 phosphorylation and p21Cip/WAK-1. J Biol Chem 2004;279:49199–205.
[61] Cao Q, Zhang L, Yang G, Xu C, Wang R. Butyrate-stimulated H_2S production in colon cancer cells. Antioxid Redox Signal 2010;12:1101–9.
[62] Osipov RM, Robich MP, Feng J, Liu Y, Clements RT, Glazer HP, et al. Effect of hydrogen sulfide in a porcine model of myocardial ischemia-reperfusion: comparison of different administration regimens and characterization of the cellular mechanisms of protection. J Cardiovasc Pharmacol 2009;54:287–97.
[63] Osipov RM, Robich MP, Feng J, Chan V, Clements RT, Deyo RJ, et al. Effect of hydrogen sulfide on myocardial protection in the setting of cardioplegia and cardiopulmonary bypass. Interact Cardiovasc Thorac Surg 2010;10:506–12.
[64] Szabo C, Kiss L, Pankotai E. Cytoprotective and antiinflammatory effects of hydrogen sulfide in macrophages and in mice. Crit Care 2007;11:P2.
[65] Zhang H, Zhi L, Moore PK, Bhatia M. Role of hydrogen sulfide in cecal ligation and puncture induced sepsis in the mouse. Am J Physiol Lung Cell Mol Physiol 2006;290:L1193–201.
[66] Zhu YZ, Wang ZJ, Ho P, Loke YY, Zhu YC, Huang SH, et al. Hydrogen sulfide and its possible roles in myocardial ischemia in experimental rats. J Appl Physiol 2007;102:261–8.
[67] Fiorucci S, Antonelli E, Distrutti E, Rizzo G, Mencarelli A, Orlandi S, et al. Inhibition of hydrogen sulfide generation contributes to gastric injury caused by anti-inflammatory nonsteroidal drugs. Gastroenterology 2005;129:1210–24.
[68] Bian JS, Yong QC, Pan TT, Feng ZN, Ali MY, Zhou S, et al. Role of hydrogen sulfide in the cardioprotection caused by ischemic preconditioning in the rat heart and cardiac myocytes. J Pharmacol Exp Ther 2006;316:670–8.
[69] Johansen D, Ytrehus K, Baxter GF. Exogenous hydrogen sulfide (H_2S) protects against regional myocardial ischemia–reperfusion injury—evidence for a role of K ATP channels. Basic Res Cardiol 2006;101:53–60.
[70] Oh GS, Pae HO, Lee BS, Kim BN, Kim JM, Kim HR, et al. Hydrogen sulfide inhibits nitric oxide production and nuclear factor-kappaB via heme oxygenase-1 expression in RAW264.7 macrophages stimulated with lipopolysaccharide. Free Radic Biol Med 2006;41:106–19.
[71] Biswas DK, Shi Q, Baily S, Strickland I, Ghosh S, Pardee AB, et al. NF-kappa B activation in human breast cancer specimens and its role in cell proliferation and apoptosis. Proc Natl Acad Sci USA 2004;101:10137–42.
[72] Frantzias J, Logan JG, Mollat P, Sparatore A, Del Soldato P, Ralston SH, et al. Hydrogen sulfide-releasing diclofenac derivatives inhibit breast cancer-induced osteoclastogenesis in vitro and prevent osteolysis ex vivo. Br J Pharmacol 2011. doi: 10.1111/j.1476-5381.2011.01704.x.
[73] Brennan P, O'Neill LA. Inhibition of nuclear factor kappaB by direct modification in whole cells—mechanism of action of nordihydroguaiaritic acid, curcumin and thiol modifiers. Biochem Pharmacol 1998;55:965–73.
[74] Heilman JM, Burke TJ, McClain CJ, Watson WH. Transactivation of gene expression by NF-kappaB is dependent on thioredoxin reductase activity. Free Radic Biol Med 2011;51:1533–42.
[75] Vad NM, Yount G, Moridani MY. Biochemical mechanism of acetylsalicylic acid (aspirin) selective toxicity toward melanoma cell lines. Melanoma Res 2008;18:386–99.
[76] Tesei A, Zoli W, Fabbri F, Leonetti C, Rosetti M, Bolla M, et al. NCX 4040, an NO-donating acetylsalicylic acid derivative: efficacy and mechanisms of action in cancer cells. Nitric Oxide 2008;19:225–36.
[77] Klaunig JE, Xu Y, Isenberg JS, Bachowski S, Kolaja KL, Jiang J, et al. The role of oxidative stress in chemical carcinogenesis. Environ Health Perspect 1998;106(Suppl. 1):289–95.
[78] Kiessling MK, Klemke CD, Kaminski MM, Galani IE, Krammer PH, Gulow K. Inhibition of constitutively activated nuclear factor-kappaB induces reactive oxygen species- and iron-dependent cell death in cutaneous T-cell lymphoma. Cancer Res 2009;69:2365–74.